

Radical-Initiated Formation of Aromatic Organosulfates and Sulfonates in the Aqueous Phase

Liubin Huang, Tongshan Liu, and Vicki H. Grassian*



Cite This: *Environ. Sci. Technol.* 2020, 54, 11857–11864



Read Online

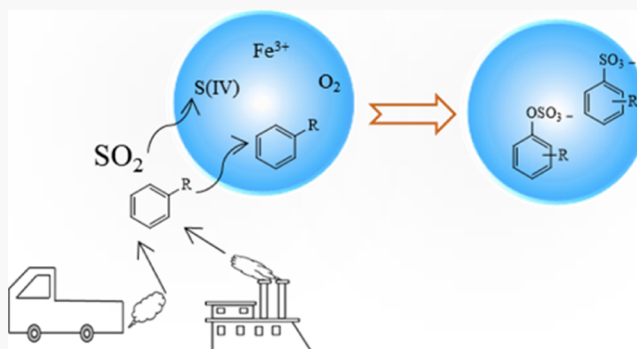
ACCESS |

Metrics & More

Article Recommendations

Supporting Information

ABSTRACT: Aromatic organosulfates and sulfonates have recently been observed in ambient aerosols collected in urban sites. Anthropogenic volatile organic compounds including aromatics are considered as their precursors in the atmosphere, but the mechanism for the formation of these compounds is still not adequately understood. In the present study, we investigated the aqueous phase reactions of benzoic acid with sulfite in the presence of Fe^{3+} under various conditions. Aromatic organosulfates and sulfonates [hereafter called aromatic organosulfur compounds (AOSCs)] can be formed during the reaction. The yield was measured as $7.3 \pm 0.6\%$, suggesting that the formation of AOSCs may provide an additional pathway for the fate of benzoic acid in the atmosphere. The mechanism for AOSC formation is proposed to be through the combination of organic radical intermediates with sulfoxide radicals, that is, SO_3^- and SO_4^- radicals. In addition to benzoic acid, other monocyclic aromatics (i.e., benzene, toluene, salicylic acid, benzyl alcohol, and phenol) can also undergo analogous mechanisms to produce various AOSCs. Interestingly, AOSC formation through this pathway can retain the aromatic ring of parent aromatics, shedding light on the fact that monocyclic aromatics can also serve as the hitherto unrecognized precursors of AOSCs in the atmosphere. Our findings provide new insights into potential sources and pathways for AOSC formation in the atmosphere.



INTRODUCTION

Atmospheric aerosols play a significant role in climate, atmospheric chemistry, and air quality.¹ Atmospheric aerosols can also have adverse impacts on human health.² A major component of submicron aerosols is organic aerosol (OA), comprising up to 20–90% of particle mass.³ OA can be directly emitted from human activities (e.g., fossil fuel combustion, biofuel burning, and cooking) as primary OA⁴ or formed as secondary OA (SOA) in the atmosphere through the oxidation of biogenic (e.g., isoprene and monoterpenes) and anthropogenic (e.g., aromatics) volatile organic compounds (VOCs) by atmospheric oxidants (e.g., O_3 , OH , and NO_3 radicals).⁵

Organosulfates are ubiquitous in atmospheric aerosols and are considered as important tracers of SOA.^{6–12} Among the most quantified and identified organosulfates are those derived from isoprene, monoterpenes, and their oxidation products.^{6,7,9–12} Laboratory studies have provided several insights into biogenic VOC-derived organosulfate formation: uptake of biogenic VOC-derived epoxides on acidic sulfate aerosols;^{13–15} sulfate radical-initiated reactions;^{16–20} substitution reaction of organonitrate by sulfate,^{21,22} and oxidation of SO_2 by organic peroxides.^{23,24}

In addition to biogenic organosulfates, aromatic organosulfates have also been detected in ambient aerosols collected

in urban sites.^{25–30} Kundu et al.²⁵ quantified the concentration of benzyl sulfate in $\text{PM}_{2.5}$ collected in Lahore, Pakistan, as 0.05 – 0.50 ng m^{-3} . Huang et al.³⁰ reported that phenyl sulfate and benzyl sulfate are the major aromatic organosulfates in $\text{PM}_{2.5}$ in Xi'an, China. The concentration of phenyl sulfate and benzyl sulfate was measured as 0.14 and 0.04 ng m^{-3} , respectively. Ma et al.²⁶ measured that the contribution of benzyl sulfate to the total identified organosulfates could be up to $\sim 63\%$ in Shanghai, China. Aromatic organosulfates seem to become more significant when anthropogenic VOCs appear to be the dominant source of SOA. Laboratory studies have revealed that aromatic organosulfates can be produced from the interaction of aromatics with sulfur-containing species.^{31,32} Riva et al.³¹ observed the formation of organosulfates and sulfonates from the photo-oxidation of polycyclic aromatic hydrocarbons (PAHs, i.e., naphthalene and 2-methylnaphthalene) in the presence of sulfate aerosols. Blair et al.³² detected a

Received: August 21, 2020

Revised: September 4, 2020

Accepted: September 9, 2020

Published: September 24, 2020



number of aromatic organosulfur species in SOA particles formed from the photo-oxidation of diesel fuel with SO_2 . However, the detailed mechanism for aromatic organosulfate formation was not determined in these studies. However, the photo-oxidation of monocyclic aromatics (e.g., toluene) under conditions that observing organosulfate formation from biogenic VOC (e.g., methacrolein) photo-oxidation,³³ did not produce detectable aromatic organosulfates.²⁷ Monocyclic aromatics were not regarded as aromatic organosulfate precursors via this pathway because they were converted to ring-opened products.^{27,34} Furthermore, it seems that current known pathways for biogenic organosulfate formation do not adequately explain the formation of detected aromatic organosulfates in the atmosphere.²⁵ Despite the fact that aromatic organosulfates have been ubiquitously observed in field and laboratory studies, their sources and formation pathways are still not fully understood.

Previous studies suggested that aqueous phase reactions and heterogeneous chemistry are efficient pathways for organosulfate formation.^{13–24,35,36} For instance, it was found that organosulfates can be generated from the aqueous phase reactions of methacrolein (MACR) and methyl vinyl ketone (MVK) with SO_4^- radicals.^{17–20} The SO_4^- radical is one of the major intermediates in the autoxidation of S(IV) catalyzed by transition metal ions (TMIs), for example, Fe^{3+} and Mn^{2+} ,³⁷ which is known to be an important pathway for sulfate formation in the atmosphere.^{38,39} The mechanism proposed involves the addition of sulfate radicals to the carbon–carbon double bonds (C=C) of MVK and MACR as shown in R1.^{17–20} It is noted that the SO_4^- radical can also react with aromatics through an electron transfer process that proceeds through a different mechanism (R2).⁴⁰



However, the formation of organosulfates, particularly for aromatic organosulfates, from this pathway is yet to be investigated.

Therefore, in this study, the aqueous phase reactions of several monocyclic aromatics with sulfite in the presence of Fe^{3+} were investigated. Benzoic acid and other abundant atmospheric aromatics, such as benzene, toluene, salicylic acid, benzyl alcohol, and phenol, were selected as representative monocyclic aromatics for this study. Our study aims to show the mechanism for the formation of aromatic organosulfates and sulfonates from these reactions and uncover that monocyclic aromatics can serve as precursors of aromatic organosulfur compounds (AOSCs) in the atmosphere.

MATERIALS AND METHODS

Batch Reactor Experiments. Details of the experiments conducted in this study are summarized in Table 1. Aqueous phase reactions were carried out using a 100 mL custom-built quartz reactor thermostated by a water jacket. $\text{Na}_2\text{S}_2\text{O}_5$ (>97%, Alfa Aesar) was used as the source of S(IV) in the solution (R3). Solutions of various pH (2–5) containing $\text{Na}_2\text{S}_2\text{O}_5$, sodium benzoate (99.5%, Sigma-Aldrich), $\text{Fe}_2(\text{SO}_4)_3$ (97%, Sigma-Aldrich), and dissolved O_2 were introduced into the reactor for a total volume of 90 mL (exp. 1–3), and then, the reactor was sealed. The initial pH of the solution was adjusted by H_2SO_4 (1 M, Fluka). Field studies reported that the concentration of dissolved iron can vary from 0.0009 to 600

Table 1. Summary of the Different Experiments Conducted in This Study

	aromatics	conc. (mM)	sulfur species	conc. (mM)	TMI	conc. (μM)	pH
1	benzoic acid	2	$\text{Na}_2\text{S}_2\text{O}_5$	1	$\text{Fe}_2(\text{SO}_4)_3$	20	5
2	benzoic acid	2	$\text{Na}_2\text{S}_2\text{O}_5$	1	$\text{Fe}_2(\text{SO}_4)_3$	20	3
3	benzoic acid	2	$\text{Na}_2\text{S}_2\text{O}_5$	1	$\text{Fe}_2(\text{SO}_4)_3$	20	2
4	benzoic acid	0.5	$\text{Na}_2\text{S}_2\text{O}_5$	1	$\text{Fe}_2(\text{SO}_4)_3$	20	3
5			$\text{Na}_2\text{S}_2\text{O}_5$	1	$\text{Fe}_2(\text{SO}_4)_3$	20	3
6	benzoic acid	2	$\text{Na}_2\text{S}_2\text{O}_5$	1			3
7	benzoic acid	2	Na_2SO_4	2			3
8	benzoic acid	2	$\text{Na}_2\text{S}_2\text{O}_5$	1	MnSO_4	40	3
9	salicylic acid	2	$\text{Na}_2\text{S}_2\text{O}_5$	1	$\text{Fe}_2(\text{SO}_4)_3$	20	3
10	phenol	2	$\text{Na}_2\text{S}_2\text{O}_5$	1	$\text{Fe}_2(\text{SO}_4)_3$	20	3
11	benzene	2	$\text{Na}_2\text{S}_2\text{O}_5$	1	$\text{Fe}_2(\text{SO}_4)_3$	20	3
12	toluene	2	$\text{Na}_2\text{S}_2\text{O}_5$	1	$\text{Fe}_2(\text{SO}_4)_3$	20	3
13	benzyl alcohol	2	$\text{Na}_2\text{S}_2\text{O}_5$	1	$\text{Fe}_2(\text{SO}_4)_3$	20	3
14	benzoic acid	2	$\text{K}_2\text{S}_2\text{O}_8$	5			
15	salicylic acid	2	$\text{K}_2\text{S}_2\text{O}_8$	5			
16	phenol	2	$\text{K}_2\text{S}_2\text{O}_8$	5			

μM in the atmospheric aqueous phase (rain, droplet, and fog);⁴¹ thus the concentration of Fe^{3+} was determined as 40 μM in this study. The concentration of $\text{Na}_2\text{S}_2\text{O}_5$ and benzoic acid was 1 and 2 mM, respectively. The elevated benzoic acid concentration used is aimed to obtain an unambiguous signal of products in mass spectrometry; nevertheless, the reaction with lower benzoic acid concentration (0.5 mM) was also investigated (exp. 4). Several control experiments, such as the solution of $\text{Na}_2\text{S}_2\text{O}_5$ mixed with Fe^{3+} , the solution of benzoic acid mixed with $\text{Na}_2\text{S}_2\text{O}_5$ alone, the solution of benzoic acid mixed with Na_2SO_4 , were carried out (exp. 5–7). In exp. 8 in Table 1, the effect of different TMI, MnSO_4 (>99%, Acros) on AOSC formation was investigated.



In addition to benzoic acid, the reactions of other monocyclic aromatics, that is, salicylic acid (99%, Alfa Aesar), phenol (>99%, Alfa Aesar), benzyl alcohol (>99%, Fisher), benzene (99.9%, Sigma-Aldrich), and toluene (99.8%, ACROS), with $\text{Na}_2\text{S}_2\text{O}_5$ in the presence of Fe^{3+} at pH 3 were also examined (exp. 9–13). All experiments were done in the dark at 298 K in triplicate. Aliquots were extracted at the specific time for the duration of 60 min. Each ~1.5 mL of the aliquot taken was immediately added with 75 μL of formaldehyde (1 M) to quench further oxidation of S(IV). After that, samples were analyzed using ultrahigh-performance liquid chromatography (UPLC) equipped with a heated electrospray ionization–high-resolution hybrid linear ion trap mass spectrometer (HESI–HRMS Thermo Orbitrap Elite).

Additional experiments (exp. 14–16) were conducted to investigate the mechanism of aromatic organosulfate formation employing $\text{K}_2\text{S}_2\text{O}_8$ (>99%, Sigma-Aldrich) as the source of sulfate radicals. Reactions of benzoic acid, phenol, and salicylic

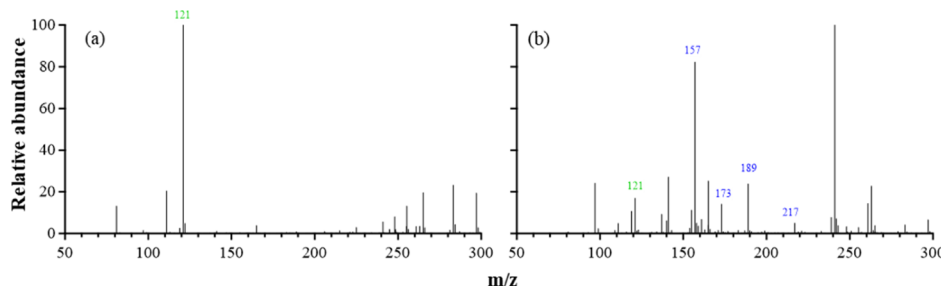


Figure 1. Mass spectra for the aqueous reaction of benzoic acid (2 mM) with $\text{Na}_2\text{S}_2\text{O}_5$ (1 mM) in the presence of Fe^{3+} (40 μM) at pH 3 acquired at (a) 0 and (b) 60 min. Peaks of benzoic acid and AOSCs are labeled with green and blue color, respectively.

acid with $\text{K}_2\text{S}_2\text{O}_8$ were carried out at 323 K without any pH control in the dark for 90 min, where sulfate radicals can be produced by heating $\text{K}_2\text{S}_2\text{O}_8$ under this condition (R4).⁴² Although the OH radical is the byproduct during $\text{SO}_4^{\cdot-}$ radical generation (R5), in a previous study, it was suggested that the concentration of produced OH radicals can be negligible.⁴³ The concentration of aromatics and $\text{K}_2\text{S}_2\text{O}_8$ was 2 and 5 mM, respectively. Similarly, the solution was extracted for UPLC-MS analysis after the reaction.



Reactants and Products Analysis. Quantitative analysis for reactants and products was performed by a UPLC/HESI-HRMS operated in the negative ionization mode. A total of 10 μL of the sample without dilution was injected into the UPLC. Products were separated by reverse-phase liquid chromatography equipped with an Acclaim OA column (4.0 \times 250 mm, 5 μm ; Thermo Fisher Scientific) at 303 K prior to mass spectrometric analysis. The isocratic elution was performed at a flow rate of 0.5 mL min^{-1} for 25 min using 70% A mobile phase (0.1% formic acid with ultrapure water) with the remaining B mobile phase (0.1% formic acid with methanol). Mass spectral data were collected in the range of m/z 100–1000, with the resolution set to 120,000. The capillary of the MS inlet was maintained at 653 K, and the S-Lens was set to 60%.

As noted above, formaldehyde (HCHO) was immediately added after solution extraction, as unreacted S(IV) can be combined with HCHO to form hydroxymethanesulfonate, corresponding to m/z 111 ($\text{CH}_3\text{SO}_4^{\cdot-}$) in the mass spectra. Therefore, the intensity of the peak at m/z 111 was used to represent the concentration of S(IV) in this study. Several commercial aromatic organosulfates and sulfonates were employed as standards for AOSC quantitation and structure identification. Phenyl sulfate (>98%, TCI, retention time (RT) 11.47) and tolyl sulfate (>98%, TCI, RT 14.52) were employed as surrogates to quantify formed aromatic organosulfates. 4-phenolsulfonic acid (99%, Acros, RT 6.03), 4-sulfobenzoic acid (98%, Acros, RT 6.43), and 2-formylbenzenesulfonic acid (>98%, Frontier Scientific, RT 8.74) salts served to quantify the amount of aromatic sulfonate formation. Their calibration curves are provided in Figure S1.

For the reaction of benzoic acid (exp. 2) or toluene (exp. 12) with $\text{Na}_2\text{S}_2\text{O}_5$ in the presence of Fe^{3+} , complementary analyses were carried out by HESI-HRMS using the direct infusion mode under the negative ionization mode. Samples were diluted by a factor of 10 with methanol (Fluka) before

analysis. The details of this method can be seen in our previous work.¹⁹ Selected products were further analyzed using MS^2 fragmentation to confirm their structures with a normalized collision energy level of 10–35 V in the range of m/z 50–500.

RESULTS AND DISCUSSION

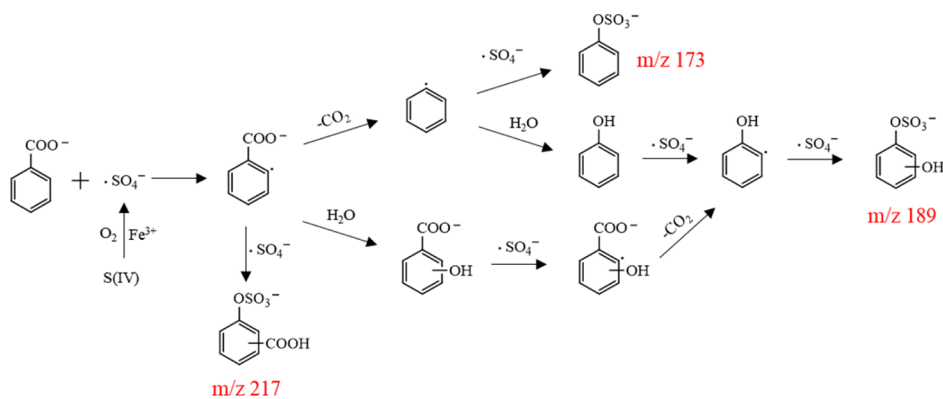
AOSC Formation from Benzoic Acid. Figure 1 shows the mass spectra for the reaction of benzoic acid with $\text{Na}_2\text{S}_2\text{O}_5$ in the presence of Fe^{3+} at pH 3 acquired at (a) 0 and (b) 60 min using the direct infusion mode. Comparison of the spectra reveals a number of products formed after the reaction. Major products containing the $\text{R}-\text{SO}_3$ or $\text{R}-\text{SO}_4^{\cdot-}$ group, that show the appearance of peaks at m/z 80 ($\text{SO}_3^{\cdot-}$), 81 ($\text{HSO}_3^{\cdot-}$), or 96 ($\text{SO}_4^{\cdot-}$) in MS^2 spectra,^{44,45} are labeled in Figure 1. Their exact mass, number of isomers, suggested formula, and possible structure are displayed in Table 2. Figure S2 presents extracted

Table 2. Exact Mass, Formula, the Number of Isomers, and the Structure of AOSCs Formed in the Reaction of Benzoic Acid with $\text{Na}_2\text{S}_2\text{O}_5$ in the Presence of Fe^{3+}

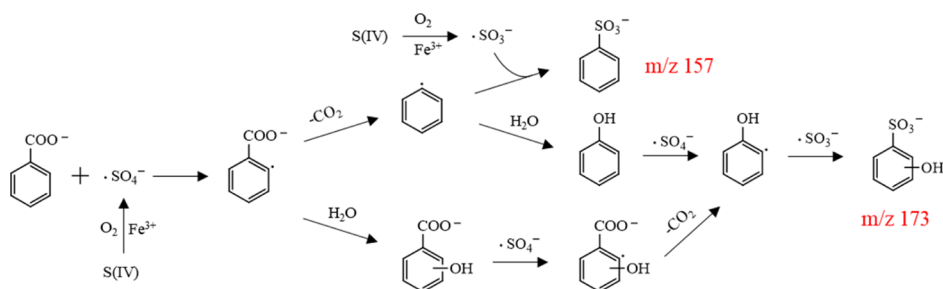
m/z [M-H] ⁻	Error (ppm)	Formula	Retention time (min)	Structure
156.99658	0.57	$\text{C}_6\text{H}_5\text{SO}_3$	7.29	
			6.03, 9.47	
172.99142	0.10	$\text{C}_6\text{H}_5\text{SO}_4$	11.47	
			7.22, 7.46, 11.68	
216.98109	-0.65	$\text{C}_7\text{H}_5\text{SO}_6$	7.14	

ion chromatograms (EICs) of these compounds, and Figure S3 shows the corresponding MS^2 spectra. The MS^2 spectrum of m/z 157 shows a peak at m/z 80 and the loss of SO_2 (m/z 93, $\text{M}-\text{SO}_2$) in accordance with the expectation of sulfonate. Thus, m/z 157 was identified as phenyl sulfonate. Three isomers were observed for m/z 173 with the formula of $\text{C}_6\text{H}_5\text{SO}_4^{\cdot-}$ (Figure S2b). Two of these isomers were identified as phenyl sulfate (RT 11.47) and 4-phenolsulfonate (RT 6.03) by the comparison with authentic standards. The remaining isomer may be a different structure of phenolsulfonate. Figure S2c displays that m/z 189 also contains three isomers. The m/z

Scheme 1. Proposed Pathways for the Formation of Aromatic Organosulfates, *m/z* 173, 189, and 217, from the Aqueous Reaction of Benzoic Acid with Sulfate Radicals



Scheme 2. Proposed Pathways for the Formation of Aromatic Sulfonates, *m/z* 157 and 189, from the Aqueous Reaction of Benzoic Acid with Sulfite and Sulfate Radicals



m/z 189 corresponds to the formula $C_6H_5SO_5^-$, which is compatible with a hydroxyphenyl sulfate or dihydroxyphenyl sulfonate. However, because of the absence of an ion at *m/z* 125 ($C_6H_5O_3^-$, $M-SO_2$) and high intensity of the fragmenting ion at *m/z* 109 ($C_6H_5O_2^-$, $M-SO_3$), indicating the loss of SO_3 as the neutral fragment, *m/z* 189 was tentatively assigned to hydroxyphenyl sulfate. The peak at *m/z* 217 with the formula of $C_7H_5SO_6^-$ reveals the benzoic acid backbone on the basis of the fragmenting ion at *m/z* 173 ($C_6H_5SO_4^-$, $M-CO_2$). The possible isobaric structure of sulfosalicylic acid was excluded by the absence of fragmenting ion at *m/z* 153 ($C_7H_5O_4^-$, $M-SO_2$), which is specific to aryl sulfonate. Thus, the assignment of *m/z* 217 was determined to be most likely benzoic sulfate. EICs shown in Figure S2 also provide the convincing evidence that these ions are the substantial products formed from the reaction rather than adducts that form because of the electrospray ionization process. The results of control experiments verify that these AOSCs cannot be generated either from the solution of benzoic acid mixed with $Na_2S_2O_5$ alone or from the solution of benzoic acid mixed with Na_2SO_4 . Therefore, the formation of these products most likely arises from the oxidation of benzoic acid by sulfoxyl radicals (i.e., SO_3^- and SO_4^- radicals) formed during the autoxidation of S(IV) catalyzed by Fe^{3+} .

The oxidation of benzoic acid by the SO_4^- radical is initiated via an electron transfer step that generates a carboxyphenyl radical intermediate. This radical can react with H_2O to form hydroxyl benzoic acid or undergo decarboxylation to produce a phenyl radical.^{46,47} Upon further reactions, the phenyl radical can be converted into phenol or other products, for example, catechol and hydroquinone.⁴³ In addition to phenol and hydroxyl benzoic acid, as mentioned above, AOSCs were also observed during the reaction. To the best of knowledge, the

formation of AOSCs has not been previously reported. Interestingly, except *m/z* 217, *m/z* 157, 173, and 189 reveal the structure that does not retain the carboxylic group, suggesting that these AOSCs are produced from phenyl radicals. The plausible pathways for the formation of observed AOSCs are proposed in Schemes 1 and 2.

Scheme 1 shows the mechanism for the formation of observed aromatic organosulfates. According to the structure of *m/z* 217, it is elucidated through the combination of the carboxyphenyl radical with the SO_4^- radical. Although the peak intensity of *m/z* 217 is weak, its appearance complements the addition pathway for the fate of the carboxyphenyl radical. Similarly, the reaction of the phenyl radical with the SO_4^- radical results in the production of phenyl sulfate (*m/z* 173). The *m/z* 189 signal shows the structure of phenyl sulfate with the substitution of a hydroxyl group (Table 2); hence, this product seems to arise from the further oxidation of phenol. It is noted that hydroxyl benzoic acid can also be the precursor of *m/z* 189 through decarboxylation followed by the combination with sulfate radicals. However, contrary to benzoic acid, decarboxylation is not the preferential pathway for the fate of hydroxyl benzoic acid oxidized by sulfate radicals.⁴⁶ The *m/z* 189 produced from hydroxyl benzoic acid may not be the major pathway for the formation of this product.

Overall, organosulfates are mainly thought to be produced from the combination of the corresponding precursor radicals with SO_4^- radicals. To verify the involvement of SO_4^- radicals, the reaction of benzoic acid with $K_2S_2O_8$ at 323 K was performed. Figure 2 shows that *m/z* 173 and 189 can also be produced from the reaction. Without pH control and other reactants added, the observation of organosulfate formation must originate from the reaction of benzoic acid with SO_4^- radicals. As discussed above, observed *m/z* 189 is speculated to

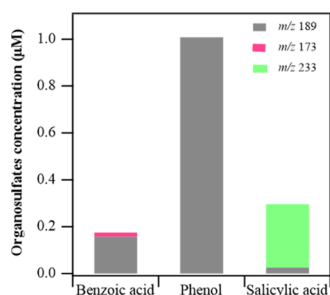


Figure 2. Concentrations of identified aromatic organosulfates (m/z 173, 189, and 233) produced from the reaction of benzoic acid, phenol, or salicylic acid with $K_2S_2O_8$ at 323 K for 90 min. The concentration of aromatics (i.e., benzoic acid, phenol, and salicylic acid) and $K_2S_2O_8$ was 2 and 5 mM, respectively.

be mainly produced from phenol rather than hydroxyl benzoic acid. Therefore, we also carried out the reactions of phenol and salicylic acid with $K_2S_2O_8$ at 323 K to validate the speculation. It is noted that m/z 233 ($C_7H_5SO_7^-$), which retains the benzoic acid backbone, is the dominant AOSC formed in the reaction of salicylic acid with SO_4^- radicals. This result demonstrates that decarboxylation is not the major pathway for hydroxyl benzoic acid degradation. Another robust evidence is that the concentration of m/z 189 produced from phenol is an order of magnitude greater than that produced from salicylic acid.

Analogous to aromatic organosulfates, the pathways for aromatic sulfonate formation shown in **Scheme 2** are elucidated through the combination of organic radicals with SO_3^- radicals. The reaction is also initiated from the oxidation of benzoic acid by SO_4^- radicals with carboxyphenyl radical production. m/z 157 and 173 are generated from the reaction of benzyl radicals and phenyl radicals with sulfite radicals, respectively. Similar to m/z 189, m/z 173 is speculated to be mainly produced from phenol rather than hydroxyl benzoic acid.

Figure 3 shows the time profile of benzoic acid and S(IV) concentrations and AOSC formation in the reaction of benzoic acid with $Na_2S_2O_5$ in the presence of Fe^{3+} at pH 3. According to the concentration of AOSCs formed and the concentration

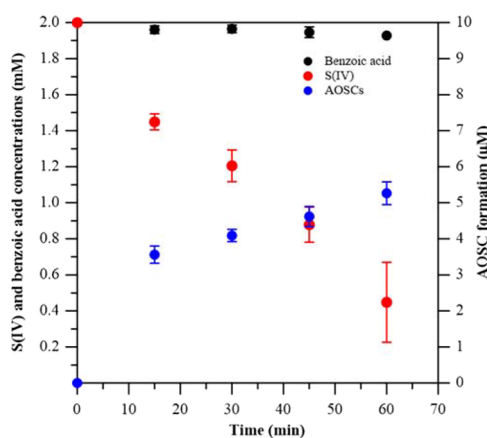


Figure 3. Time dependence of benzoic acid and S(IV) concentrations, as well as AOSC formation in the reaction of benzoic acid with $Na_2S_2O_5$ in the presence of Fe^{3+} at pH 3. Experimental conditions: $[Na_2S_2O_5] = 1$ mM; $[benzoic\ acid] = 2$ mM; $[Fe^{3+}] = 40$ μ M; $T = 25$ °C.

of S(IV) consumed after the reaction, the yield of AOSC formation from sulfur was calculated as 0.4%. Our previous work reported that the yield of OSC formation in the reaction of MVK/MACR with S(IV) in the presence of Fe^{3+} could be up to 40%.²⁰ It is noted that the value of yield is much higher from MVK/MACR than benzoic acid. This discrepancy may be attributed to the different mechanisms for the formation of OSCs between benzoic acid and MVK/MACR. OSC produced from MVK/MACR is initiated by the addition of sulfoxyl radicals to $C=C$. OSC can be directly formed in the first step (**Reaction R1**). However, as shown in **R2**, the initial step for the reaction of benzoic acid with sulfate radicals is an electron transfer, resulting in the formation of the carboxyphenyl radical and sulfate. OSC is formed via the further oxidation of the carboxyphenyl radical. The yield of AOSC formation from benzoic acid is also calculated by the ratio of the concentration of AOSC formed to the concentration of benzoic acid consumed after reaction. The yield was measured as $7.3 \pm 0.6\%$, indicating that AOSC formation may be an important pathway for the fate of benzoic acid. At 0.5 mM benzoic acid, the yield was calculated as 7.5%, which is similar to that at 2 mM benzoic acid under the same experimental conditions. Except for the formation of AOSCs, **Figure S4** shows that the reaction of benzoic acid with sulfoxyl radicals also has an impact on the S(IV) autoxidation. The autoxidation of S(IV) catalyzed by Fe^{3+} is significantly inhibited by the presence of benzoic acid, and the inhibition effect positively depends on the initial concentration of benzoic acid. This observation is consistent with the previous study which also investigated the effect of benzoic acid on S(IV) autoxidation.⁴⁸ It is noted the inhibitory effect could also be possibly caused by the decreased amount of catalytically active Fe^{3+} because of the complexation of Fe^{3+} with organic acids.⁴⁹ However, a previous study found that no detectable inner-sphere complexes were formed when Fe^{3+} was added to the solution of benzoic acid.⁵⁰ Therefore, in this study, Fe-catalyzed S(IV) autoxidation inhibited by the presence of benzoic acid may be ascribed to the scavenging of sulfoxyl radicals by benzoic acid.

Benzoic Acid-Derived AOSC Formation at Different pH Values and Different Sources of Sulfoxyl Radicals.

Given the varying range of pH values, from slightly alkaline to highly acidic, in aqueous phase environments in the atmosphere,⁵¹ the effects of pH on the formation of AOSCs were investigated. It is expected that higher solution acidity can promote the production of sulfoxyl radicals,³⁷ thereby facilitating AOSCs formation. However, conversely, the concentration of AOSCs measured at pH 5 (5.1 ± 0.1 μ M) is comparable with that at pH 3 (5.3 ± 0.3 μ M). It is noted that the fraction of protonated (C_6H_5COOH) and deprotonated ($C_6H_5COO^-$) benzoic acid is also closely related to the solution pH values. Previous studies reported that the rate constant of SO_4^- radicals reacted with CH_3COO^- is at least an order higher than that of reacted with CH_3COOH .^{52,53} Thus, in this study, the reaction of SO_4^- radicals with $C_6H_5COO^-$ may be much faster than the reaction of SO_4^- radicals with C_6H_5COOH as well. As shown in **Figure S5**, ~10% benzoic acid is in the form of $C_6H_5COO^-$ at pH 3, while this ratio increases to 70% at pH 5. Because of the higher fraction of deprotonated ($C_6H_5COO^-$) benzoic acid, although the efficiency of sulfoxyl radical production at pH 5 is lower than that at pH 3, the concentration of AOSCs at pH 5 is still comparable with that at pH 3. This may also be the possible explanation for the observation that the concentration of

AOSCs at pH 2 (0.83 μM) is much lower than that at pH 3 given that benzoic acid is fully protonated at pH 2 (Figure S5).

As shown in **Schemes 1** and **2**, AOSC formation is elucidated through the reaction of benzoic acid with sulfoxyl radicals formed from Fe-catalyzed S(IV) autoxidation. Mn^{2+} is known as another important catalyst for S(IV) autoxidation in the atmosphere.³⁷ In this study, the reaction of benzoic acid with $\text{Na}_2\text{S}_2\text{O}_5$ in the presence of Mn^{2+} at pH 3 was also performed. It was found that the concentration of AOSCs formed in the presence of Mn^{2+} ($0.10 \pm 0.01 \mu\text{M}$) was much lower than that in the presence of Fe^{3+} ($5.3 \pm 0.3 \mu\text{M}$) under the same experimental conditions. It may be partially attributed to the lower production of sulfoxyl radicals by the fact that only $\sim 20\%$ of S(IV) was consumed after 1 h reaction. Nevertheless, the observation of AOSCs formed in the presence of Mn^{2+} further demonstrates that sulfoxyl radicals play an important role in AOSC formation.

AOSC Formation from Other Monocyclic Aromatics.

In addition to benzoic acid, AOSC formation from other monocyclic aromatics was also examined (exp. 9–13). Figure S6a shows the mass spectrum for the reaction of toluene with $\text{Na}_2\text{S}_2\text{O}_5$ in the presence of Fe^{3+} . m/z 171 and 187 were the major AOSCs produced during the reaction. The weak peak at m/z 171 ($\text{C}_7\text{H}_7\text{SO}_3^-$) was speculated as arylsulfonate. Two isomers were observed for m/z 187 with the formula of $\text{C}_7\text{H}_7\text{SO}_4^-$. One of the isomers was established as tolyl sulfate by the comparison with the authentic standard. It is noted that MS^2 spectrum of m/z 187 displays a distinct fragmentation peak at m/z 96 (SO_4^-) (Figure S6b). This peak cannot arise from tolyl sulfate because the elimination of sulfate radicals is less favorable when the sulfate functional group is directly attached to the aromatic ring.⁴⁴ Thus, another isomer of $\text{C}_7\text{H}_7\text{SO}_4^-$ was inferred as benzyl sulfate that can produce the fragmentation ion at m/z 96. Scheme S1 shows possible pathways for the formation of tolyl sulfate and benzyl sulfate via the reaction of toluene with sulfate radicals. Additionally, other monocyclic aromatics investigated can also undergo analogous mechanisms as proposed for benzoic acid to produce corresponding AOSCs. This observation suggests that this sulfoxyl radical-involving mechanism can be potentially applied for other aromatic compounds in the atmosphere. The concentration of AOSCs produced from the reaction of different monocyclic aromatics (i.e., salicylic acid, benzoic acid, benzyl alcohol, benzene, toluene, and phenol) with $\text{Na}_2\text{S}_2\text{O}_5$ in the presence of Fe^{3+} at pH 3 is shown in Figure 4. The pronounced difference in terms of the concentration of AOSCs formed between different aromatics was found. This difference cannot be fully ascribed to their different reactivity toward sulfate radicals. For instance, the rate constant ($k_{\text{SO}_4^{\bullet-}}$) of benzene and toluene with sulfate radicals was reported as $(6.4 \pm 2.5) \times 10^8 \text{ L M}^{-1} \text{ s}^{-1}$ and $(1.3 \pm 0.6) \times 10^9 \text{ L M}^{-1} \text{ s}^{-1}$, respectively.⁵⁴ However, the concentration of organosulfur compounds produced from toluene is ~ 20 times larger than that produced from benzene. The possible explanation for these differences is not clear, and further study is warranted.

Atmospheric Implication and Conclusions. The current study reveals a plausible mechanism for AOSC formation through the aqueous phase reactions of monocyclic aromatics with sulfite in the presence of Fe^{3+} . The mechanism is elucidated by the combination of organic radical intermediates with sulfate or sulfite radicals. AOSCs formed through this pathway can retain the aromatic ring of parent

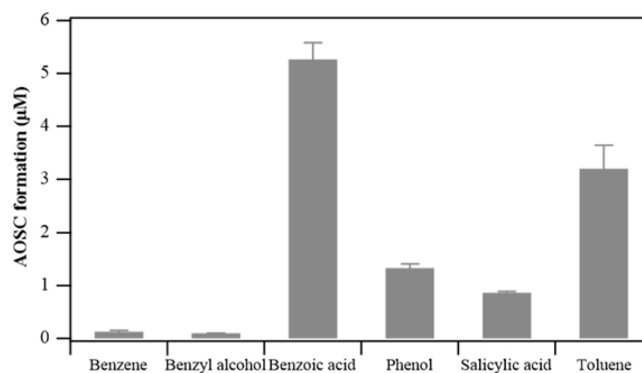


Figure 4. Concentration of AOSCs produced from the reaction of different monocyclic aromatics (2 mM, i.e., benzene, benzyl alcohol, benzoic acid, phenol, salicylic acid, and toluene) with $\text{Na}_2\text{S}_2\text{O}_5$ (1 mM) in the presence of Fe^{3+} (40 μM) at pH 3 for 60 min.

aromatics, shedding light on that monocyclic aromatics, for example, toluene, can also serve as the hitherto unrecognized precursors for aromatic AOSCs in addition to PAHs.³¹ Many of AOSCs, such as phenyl sulfate (m/z 173) and benzyl sulfate (m/z 187) identified in this study were also observed in ambient aerosols collected in urban sites,^{25,27,29,30} suggesting that aromatic oxidation by sulfoxyl radicals may be the potential source for AOSC formation in the atmosphere. Further investigations about extrapolating these reactions from bulk to the aerosol phase and evaluating the importance of these reactions in the atmosphere are warranted.

ASSOCIATED CONTENT

Supporting Information

The Supporting Information is available free of charge at <https://pubs.acs.org/doi/10.1021/acs.est.0c05644>.

Calibration curve of standards; EICs and MS^2 spectra of observed AOSCs; effect of benzoic acid concentration on S(IV) catalytic oxidation; fraction of different benzoic acid forms at different pH values; mass spectrum for the reaction of toluene with sulfoxyl radicals, MS^2 spectrum of m/z 187, and proposed pathways for m/z 187 formation (PDF)

AUTHOR INFORMATION

Corresponding Author

Vicki H. Grassian – Department of Chemistry and Biochemistry, Department of Nanoengineering and Scripps Institution of Oceanography, University of California San Diego, La Jolla, California 92093, United States; orcid.org/0000-0001-5052-0045; Phone: (858)-534-2499; Email: vhgrassian@ucsd.edu

Authors

Liubin Huang – Department of Chemistry and Biochemistry, University of California San Diego, La Jolla, California 92093, United States

Tongshan Liu – Department of Chemistry and Biochemistry, University of California San Diego, La Jolla, California 92093, United States

Complete contact information is available at: <https://pubs.acs.org/10.1021/acs.est.0c05644>

Notes

The authors declare no competing financial interest.

ACKNOWLEDGMENTS

This material is based upon work supported by the National Science Foundation under grant AGS1702488.

REFERENCES

(1) Seinfeld, J. H.; Pandis, S. N. *Atmospheric Chemistry and Physics: From Air Pollution to Climate Change*, 2nd ed; Wiley: New York, 2006.

(2) Shiraiwa, M.; Ueda, K.; Pozzer, A.; Lammel, G.; Kampf, C. J.; Fushimi, A.; Enami, S.; Arango, A. M.; Fröhlich-Nowoisky, J.; Fujitani, Y.; Furuyama, A.; Lakey, P. S. J.; Lelieveld, J.; Lucas, K.; Morino, Y.; Pöschl, U.; Takahama, S.; Takami, A.; Tong, H.; Weber, B.; Yoshino, A.; Sato, K. Aerosol health effects from molecular to global scales. *Environ. Sci. Technol.* **2017**, *51*, 13545–13567.

(3) Hallquist, M.; Wenger, J. C.; Baltensperger, U.; Rudich, Y.; Simpson, D.; Claeys, M.; Dommen, J.; Donahue, N. M.; George, C.; Goldstein, A. H.; Hamilton, J. F.; Herrmann, H.; Hoffmann, T.; Iinuma, Y.; Jang, M.; Jenkin, M. E.; Jimenez, J. L.; Kiendler-Scharr, A.; Maenhaut, W.; McFiggans, G.; Mentel, T. F.; Monod, A.; Prévôt, A. S. H.; Seinfeld, J. H.; Surratt, J. D.; Szmigielski, R.; Wildt, J. The formation, properties and impact of secondary organic aerosol: current and emerging issues. *Atmos. Chem. Phys.* **2009**, *9*, 5155–5236.

(4) Shrivastava, M.; Cappa, C. D.; Fan, J.; Goldstein, A. H.; Guenther, A. B.; Jimenez, J. L.; Kuang, C.; Laskin, A.; Martin, S. T.; Ng, N. L.; Petaja, T.; Pierce, J. R.; Rasch, P. J.; Roldin, P.; Seinfeld, J. H.; Shilling, J.; Smith, J. N.; Thornton, J. A.; Volkamer, R.; Wang, J.; Worsnop, D. R.; Zaveri, R. A.; Zelenyuk, A.; Zhang, Q. Recent advances in understanding secondary organic aerosol: Implications for global climate forcing. *Rev. Geophys.* **2017**, *55*, 509–559.

(5) Jimenez, J. L.; Canagaratna, M. R.; Donahue, N. M.; Prevot, A. S. H.; Zhang, Q.; Kroll, J. H.; DeCarlo, P. F.; Allan, J. D.; Coe, H.; Ng, N. L.; Aiken, A. C.; Docherty, K. S.; Ulbrich, I. M.; Grieshop, A. P.; Robinson, A. L.; Duplissy, J.; Smith, J. D.; Wilson, K. R.; Lanz, V. A.; Hueglin, C.; Sun, Y. L.; Tian, J.; Laaksonen, A.; Raatikainen, T.; Rautiainen, J.; Vaattovaara, P.; Ehn, M.; Kulmala, M.; Tomlinson, J. M.; Collins, D. R.; Cubison, M. J.; Dunlea, J.; Huffman, J. A.; Onasch, T. B.; Alfarra, M. R.; Williams, P. I.; Bower, K.; Kondo, Y.; Schneider, J.; Drewnick, F.; Borrmann, S.; Weimer, S.; Demerjian, K.; Salcedo, D.; Cottrell, L.; Griffin, R.; Takami, A.; Miyoshi, T.; Hatakeyama, S.; Shimojo, A.; Sun, J. Y.; Zhang, Y. M.; Dzepina, K.; Kimmel, J. R.; Sueper, D.; Jayne, J. T.; Herndon, S. C.; Trimborn, A. M.; Williams, L. R.; Wood, E. C.; Middlebrook, A. M.; Kolb, C. E.; Baltensperger, U.; Worsnop, D. R. Evolution of organic aerosols in the atmosphere. *Science* **2009**, *326*, 1525–1529.

(6) Surratt, J. D.; Gómez-González, Y.; Chan, A. W. H.; Vermeylen, R.; Shahgholi, M.; Kleindienst, T. E.; Edney, E. O.; Offenberg, J. H.; Lewandowski, M.; Jaoui, M.; Maenhaut, W.; Claeys, M.; Flagan, R. C.; Seinfeld, J. H. Organosulfate formation in biogenic secondary organic aerosol. *J. Phys. Chem. A* **2008**, *112*, 8345–8378.

(7) Kristensen, K.; Glasius, M. Organosulfates and oxidation products from biogenic hydrocarbons in fine aerosols from a forest in North West Europe during spring. *Atmos. Environ.* **2011**, *45*, 4546–4556.

(8) Tolocka, M. P.; Turpin, B. Contribution of organosulfur compounds to organic aerosol mass. *Environ. Sci. Technol.* **2012**, *46*, 7978–7983.

(9) Stone, E. A.; Yang, L.; Yu, L. E.; Rupakheti, M. Characterization of organosulfate in atmospheric aerosols at four Asian locations. *Atmos. Environ.* **2012**, *47*, 323–329.

(10) He, Q.-F.; Ding, X.; Wang, X.-M.; Yu, J.-Z.; Fu, X.-X.; Liu, T.-Y.; Zhang, Z.; Xue, J.; Chen, D.-H.; Zhong, L.-J.; Donahue, N. M. Organosulfates from pinene and isoprene over the Pearl River Delta, South China: seasonal variation and implication in formation mechanisms. *Environ. Sci. Technol.* **2014**, *48*, 9236–9245.

(11) Hansen, A. M. K.; Kristensen, K.; Nguyen, Q. T.; Zare, A.; Cozzi, F.; Nørgaard, J. K.; Skov, H.; Brandt, J.; Christensen, J. H.; Ström, J.; Tunved, P.; Krejci, R.; Glasius, M. Organosulfates and organic acids in Arctic aerosols: Speciation, annual variation and concentration levels. *Atmos. Chem. Phys.* **2014**, *14*, 7807–7823.

(12) Wang, Y.; Hu, M.; Guo, S.; Wang, Y.; Zheng, J.; Yang, Y.; Zhu, W.; Tang, R.; Li, X.; Liu, Y.; Le Breton, M.; Du, Z.; Shang, D.; Wu, Y.; Wu, Z.; Song, Y.; Lou, S.; Hallquist, M.; Yu, J. The secondary formation of organosulfates under interactions between biogenic emissions and anthropogenic pollutants in summer in Beijing. *Atmos. Chem. Phys.* **2018**, *18*, 10693–10713.

(13) Riva, M.; Chen, Y.; Zhang, Y.; Lei, Z.; Olson, N. E.; Boyer, H. C.; Narayan, S.; Yee, L. D.; Green, H. S.; Cui, T.; Zhang, Z.; Baumann, K.; Fort, M.; Edgerton, E.; Budisulistiorini, S. H.; Rose, C. A.; Ribeiro, I. O.; Oliveira, R. L.; dos Santos, E. O.; Machado, C. M. D.; Szopa, S.; Zhao, Y.; Alves, E. G.; de Sá, S. S.; Hu, W.; Knipping, E. M.; Shaw, S. L.; Duvoisin Junior, S.; de Souza, R. A. F.; Palm, B. B.; Jimenez, J.-L.; Glasius, M.; Goldstein, A. H.; Pye, H. O. T.; Gold, A.; Turpin, B. J.; Vizuete, W.; Martin, S. T.; Thornton, J. A.; Dutcher, C. S.; Ault, A. P.; Surratt, J. D. Increasing isoprene epoxydiol-to-inorganic sulfate aerosol ratio results in extensive conversion of inorganic sulfate to organosulfur forms: implications for aerosol physicochemical properties. *Environ. Sci. Technol.* **2019**, *53*, 8682–8694.

(14) Surratt, J. D.; Chan, A. W. H.; Eddingsaas, N. C.; Chan, M.; Loza, C. L.; Kwan, A. J.; Hersey, S. P.; Flagan, R. C.; Wennberg, P. O.; Seinfeld, J. H. Reactive intermediates revealed in secondary organic aerosol formation from isoprene. *Proc. Natl. Acad. Sci. U.S.A.* **2010**, *107*, 6640–6645.

(15) Drozd, G. T.; Woo, J. L.; McNeill, V. F. Self-limited uptake of α -pinene oxide to acidic aerosol: the effects of liquid-liquid phase separation and implications for the formation of secondary organic aerosol and organosulfates from epoxides. *Atmos. Chem. Phys.* **2013**, *13*, 8255–8263.

(16) Rudziński, K. J.; Gmachowski, L.; Kuznietsova, I. Reactions of isoprene and sulphonyl radical-anions—a possible source of atmospheric organosulphites and organosulphates. *Atmos. Chem. Phys.* **2009**, *9*, 2129–2140.

(17) Nozière, B.; Ekström, S.; Alsberg, T.; Holmström, S. Radical-initiated formation of organosulfates and surfactants in atmospheric aerosols. *Geophys. Res. Lett.* **2010**, *37*. DOI: 10.1029/2009gl041683

(18) Schindelka, J.; Iinuma, Y.; Hoffmann, D.; Herrmann, H. Sulfate radical-initiated formation of isoprene-derived organosulfates in atmospheric aerosols. *Faraday Discuss.* **2013**, *165*, 237–259.

(19) Huang, L.; Cochran, R. E.; Coddens, E. M.; Grassian, V. H. Formation of organosulfur compounds through transition metal ion-catalyzed aqueous phase reactions. *Environ. Sci. Technol. Lett.* **2018**, *5*, 315–321.

(20) Huang, L.; Coddens, E. M.; Grassian, V. H. Formation of organosulfur compounds from aqueous phase reactions of S(IV) with methacrolein and methyl vinyl ketone in the presence of transition metal ions. *ACS Earth Space Chem.* **2019**, *3*, 1749–1755.

(21) Darer, A. I.; Cole-Filipliak, N. C.; O'Connor, A. E.; Elrod, M. J. Formation and stability of atmospherically relevant isoprene derived organosulfates and organonitrates. *Environ. Sci. Technol.* **2011**, *45*, 1895–1902.

(22) Hu, K. S.; Darer, A. I.; Elrod, M. J. Thermodynamics and kinetics of the hydrolysis of atmospherically relevant organonitrates and organosulfates. *Atmos. Chem. Phys.* **2011**, *11*, 8307–8320.

(23) Wang, S.; Zhou, S.; Tao, Y.; Tsui, W. G.; Ye, J.; Yu, J. Z.; Murphy, J. G.; McNeill, V. F.; Abbott, J. P. D.; Chan, A. W. H. Organic peroxides and sulfur dioxide in aerosol: source of particulate sulfate. *Environ. Sci. Technol.* **2019**, *53*, 10695–10704.

(24) Ye, J.; Abbott, J. P. D.; Chan, A. W. H. Novel pathway of SO_2 oxidation in the atmosphere: reactions with monoterpene ozonolysis intermediates and secondary organic aerosol. *Atmos. Chem. Phys.* **2018**, *18*, 5549–5565.

(25) Kundu, S.; Quraishi, T. A.; Yu, G.; Suarez, C.; Keutsch, F. N.; Stone, E. A. Evidence and quantification of aromatic organosulfates in ambient aerosols in Lahore, Pakistan. *Atmos. Chem. Phys.* **2013**, *13*, 4865–4875.

(26) Ma, Y.; Xu, X.; Song, W.; Geng, F.; Wang, L. Seasonal and diurnal variations of particulate organosulfates in urban Shanghai, China. *Atmos. Environ.* **2014**, *85*, 152–160.

(27) Staudt, S.; Kundu, S.; Lehmler, H.-J.; He, X.; Cui, T.; Lin, Y.-H.; Kristensen, K.; Glasius, M.; Zhang, X.; Weber, R. J.; Surratt, J. D.; Stone, E. A. Aromatic organosulfates in atmospheric aerosols: Synthesis, characterization, and abundance. *Atmos. Environ.* **2014**, *94*, 366–373.

(28) Tao, S.; Lu, X.; Levac, N.; Bateman, A. P.; Nguyen, T. B.; Bones, D. L.; Nizkorodov, S. A.; Laskin, J.; Laskin, A.; Yang, X. Molecular characterization of organosulfates in organic aerosols from Shanghai and Los Angeles urban areas by nanospray-desorption electrospray ionization high-resolution mass spectrometry. *Environ. Sci. Technol.* **2014**, *48*, 10993–11001.

(29) Kuang, B. Y.; Lin, P.; Hu, M.; Yu, J. Z. Aerosol size distribution characteristics of organosulfates in the Pearl River Delta region, China. *Atmos. Environ.* **2016**, *130*, 23–35.

(30) Huang, R. J.; Cao, J. J.; Chen, Y.; Yang, L.; Shen, J. C.; You, Q. H.; Wang, K.; Lin, C. S.; Xu, W.; Gao, B.; Li, Y. J.; Chen, Q.; Hoffmann, T.; O'Dowd, C. D.; Bilde, M.; Glasius, M. Organosulfates in atmospheric aerosol: synthesis and quantitative analysis of $PM_{2.5}$ from Xi'an, northwestern China. *Atmos. Meas. Tech.* **2018**, *11*, 3447–3456.

(31) Riva, M.; Tomaz, S.; Cui, T.; Lin, Y.-H.; Perraudin, E.; Gold, A.; Stone, E. A.; Villenave, E.; Surratt, J. D. Evidence for an unrecognized secondary anthropogenic source of organosulfates and sulfonates: Gasphase oxidation of polycyclic aromatic hydrocarbons in the presence of sulfate aerosol. *Environ. Sci. Technol.* **2015**, *49*, 6654–6664.

(32) Blair, S. L.; MacMillan, A. C.; Drozd, G. T.; Goldstein, A. H.; Chu, R. K.; Pasa-Tolic, N.; Tolic, L. S. J. B.; Lin, P.; Laskin, J.; Laskin, A.; Nizkorodov, S. A.; Shaw, J. B. Molecular characterization of organosulfur compounds in biodiesel and diesel fuel secondary organic aerosol. *Environ. Sci. Technol.* **2017**, *51*, 119–127.

(33) Zhang, H. F.; Lin, Y. H.; Zhang, Z. F.; Zhang, X. L.; Shaw, S. L.; Knipping, E. M.; Weber, R. J.; Gold, A.; Kamens, R. M.; Surratt, J. D. Secondary organic aerosol formation from methacrolein photo-oxidation: roles of NO_x level, relative humidity and aerosol acidity. *Environ. Chem.* **2012**, *9*, 247–262.

(34) Kamens, R. M.; Zhang, H.; Chen, E. H.; Zhou, Y.; Parikh, H. M.; Wilson, R. L.; Galloway, K. E.; Rosen, E. P. Secondary organic aerosol formation from toluene in an atmospheric hydrocarbon mixture: water and particle seed effects. *Atmos. Environ.* **2011**, *45*, 2324–2334.

(35) Iinuma, Y.; Müller, C.; Berndt, T.; Böge, O.; Claeys, M.; Herrmann, H. Evidence for the existence of organosulfates from β -pinene ozonolysis in ambient secondary organic aerosol. *Environ. Sci. Technol.* **2007**, *41*, 6678–6683.

(36) Surratt, J. D.; Kroll, J. H.; Kleindienst, T. E.; Edney, E. O.; Claeys, M.; Sorooshian, A.; Ng, N. L.; Offenberg, J. H.; Lewandowski, M.; Jaoui, M.; Flagan, R. C.; Seinfeld, J. H. Evidence for organosulfates in secondary organic aerosol. *Environ. Sci. Technol.* **2007**, *41*, 517–527.

(37) Brandt, C.; Van Eldik, R. Transition metal-catalyzed oxidation of sulfur (IV) oxides. Atmospheric-relevant processes and mechanisms. *Chem. Rev.* **1995**, *95*, 119–190.

(38) Alexander, B.; Park, R. J.; Jacob, D. J.; Gong, S. Transition metal-catalyzed oxidation of atmospheric sulfur: global implications for the sulfur budget. *J. Geophys. Res. Atmos.* **2009**, *114*, No. . DOI: 10.1029/2008jd010486

(39) Harris, E.; Sinha, B.; van Pinxteren, D.; Tilgner, A.; Fomba, K. W.; Schneider, J.; Roth, A.; Gnauk, T.; Fahlbusch, B.; Mertes, S. Enhanced role of transition metal ion catalysis during in-cloud oxidation of SO₂. *Science* **2013**, *340*, 727–730.

(40) Neta, P.; Madhavan, V.; Zemel, H.; Fessenden, R. W. Rate constants and mechanism of reaction of SO₄²⁻ with aromatic compounds. *J. Am. Chem. Soc.* **1977**, *99*, 163–164.

(41) Deguillaume, L.; Leriche, M.; Desboeufs, K.; Mailhot, G.; George, C.; Chaumerliac, N. Transition metals in atmospheric liquid phases: sources, reactivity, and sensitive parameters. *Chem. Rev.* **2005**, *105*, 3388–3431.

(42) Kolthoff, I. M.; Miller, I. K. The chemistry of persulfate. I. The kinetics and mechanism of the decomposition of the persulfate ion in aqueous medium. *J. Am. Chem. Soc.* **1951**, *73*, 3055–3059.

(43) Zrinyi, N.; Pham, A. L.-T. Oxidation of benzoic acid by heat-activated persulfate: effect of temperature on transformation pathway and product distribution. *Water Res.* **2017**, *120*, 43–51.

(44) Attygalle, A. B.; Garcia-Rubio, S.; Ta, J.; Meinwald, J. Collisionally-induced dissociation mass spectra of organic sulfate anions. *J. Chem. Soc.* **2001**, *4*, 498–506.

(45) Jariwala, F. B.; Wood, R. E.; Nishshanka, U.; Attygalle, A. B. Formation of the bisulfite anion (HSO₃⁻, m/z 81) upon collision-induced dissociation of anions derived from organic sulfonic acids. *J. Mass Spectrom.* **2012**, *47*, 529–538.

(46) Madhavan, V.; Levanon, H.; Neta, P. Decarboxylation by SO₄²⁻ radicals. *Radiat. Res.* **1978**, *76*, 15–22.

(47) Zemel, H.; Fessenden, R. W. The mechanism of reaction of sulfate radical anion with some derivatives of benzoic acid. *J. Phys. Chem.* **1978**, *82*, 2670–2676.

(48) Meena, V. K.; Dhayal, Y.; Rathore, D. S.; Chandel, C. P.; Gupta, K. S. Inhibition of atmospheric aqueous phase autoxidation of sulphur dioxide by volatile organic compounds: mono-, di- and tri-substituted benzenes and benzoic acids. *Prog. React. Kinet.* **2017**, *42*, 111–125.

(49) Grgic, I.; Dovzan, A.; Bercic, G.; Hudnik, V. The effect of atmospheric organic compounds on the Fe-catalyzed S(IV) autoxidation in aqueous solution. *J. Atmos. Chem.* **1998**, *29*, 315–337.

(50) Deng, Y. W.; Zhang, K.; Chen, H.; Wu, T. X.; Krzyaniak, M.; Wellons, A.; Bolla, D.; Douglas, K.; Zuo, Y. G. Iron-catalyzed photochemical transformation of benzoic acid in atmospheric liquids: Product identification and reaction mechanisms. *Atmos. Environ.* **2006**, *40*, 3665–3676.

(51) Pye, H. O. T.; Nenes, A.; Alexander, B.; Ault, A.; Barth, M.; Clegg, S.; Collett, J.; Fahey, K.; Hennigan, C.; Herrmann, H.; Kanakidou, M.; Kelly, J.; Ku, I.; McNeill, V. F.; Riemer, N.; Schaefer, T.; Shi, G.; Tilgner, A.; Walker, J. T.; Wang, T.; Weber, R.; Xing, J.; Zaveri, R.; Zuent, Z. The acidity of atmospheric particles and clouds. *Atmos. Chem. Phys.* **2020**, *20*, 4809–4888.

(52) Herrmann, H.; Ervens, B.; Jacobi, H. W.; Wolke, R.; Nowacki, P.; Zellner, R. CAPRAM 2.3: a chemical aqueous phase radical mechanism for tropospheric chemistry. *J. Atmos. Chem.* **2000**, *36*, 231–284.

(53) Criquet, J.; Leitner, N. K. V. Degradation of acetic acid with sulfate radical generated by persulfate ions photolysis. *Chemosphere* **2009**, *77*, 194–200.

(54) Herrmann, H.; Exner, M.; Jacobi, H. W.; Raabe, G.; Reese, A.; Zellner, R. Laboratory studies of atmospheric aqueous-phase free radical chemistry: kinetic and spectroscopic studies of reactions of NO₃ and SO₄²⁻ radicals with aromatic compounds. *Faraday Discuss.* **1995**, *100*, 129–153.